Available online at www.sciencedirect.com
ScienceDirect
Sedimentary Geology 191 (2006) 171–189
Sedimentary Geology
www.elsevier.com/locate/sedgeo

Accessory minerals in cassiterite: A tool for provenance and environmental analyses of colluvial–fluvial placer deposits (NE Bavaria, Germany)

H.G. Dill [a,*], F. Melcher [a], M. Füßl [b], B. Weber [c]

[a] *Federal Institute for Geosciences and Natural Resources, P.O. Box 510163 D-30631 Hannover, Germany*
[b] *A.-v.-Humboldt-Str. 4, D-92711 Parkstein, Germany*
[c] *Bürgermeister-Knorr Str. 8 D-92637 Weiden i.d.OPf., Germany*

Received 16 September 2005; received in revised form 15 March 2006; accepted 22 March 2006

Abstract

In general heavy minerals are used for analysis of the depositional environment and to identify source areas of grains. To give an idea of the lithology in the provenance area petrographic microscopy may provide sufficient first-hand information, but for a more detailed study electronmicroprobe analysis of solid solution series is necessary (e.g. garnet, amphibole or phosphate minerals). In the present study, mineral aggregates of cassiterite from colluvial to fluvial Sn–Ti placers in the NE Bavarian Basement, Germany, were investigated for their accessory minerals. Cassiterite aggregates contain a wide range of inclusions of Ti–Nb–Fe minerals which may help constrain the source rock. Fissures intersecting the mineral aggregates are filled with Ti-oxide hydroxides and aluminum phosphates. These phosphates were also found associated with kaolinite and anatase, lining cavities and vugs in the cassiterite clusters. The remaining pore space in the cassiterite aggregates was filled with an "internal sediment" similar to that known from calcareous rocks. Based on the variability of these accessory minerals six processes operative during or prior to placer evolution may be defined: (1) pegmatitic–hydrothermal granitic source rock evolution, (2) peneplanation and formation of paleoplacers, (3) chemical weathering and replacement of preexisting oxides and phosphates, (4) neomorphism, (5) internal sedimentation, (6) colluvial–fluvial placer deposition. Using the accessory minerals hosted by cassiterite, the physico-chemical conditions in the provenance area and in the depositional environment may be defined. The source rocks delivering the cassiterite minerals are of Late Paleozoic age. Placer formation lasted from the Late Cretaceous through the Recent.

Keywords: Cassiterite; Placer; Accessory minerals; Mesozoic–Cenozoic; NE Bavaria (Germany)

1. Introduction

Heavy mineral analysis is widely used in sedimentology, to unravel the source of clastic sediments, to assess the variation in secondary porosity during deep burial and shed some light on the weathering processes in the source area as well as in the depositional environment. For routine provenance analyses, the petrographic microscope may provide enough information (Dill, 1998). To draw a more detailed picture of the source area or carry out quantitative analysis, microchemical methods using the electronmicroprobe (EMP) are needed (Morton, 1991; Zack et al., 2004).

* Corresponding author.
E-mail address: dill@bgr.de (H.G. Dill).

0037-0738/$ - see front matter © 2006 Elsevier B.V. All rights reserved.
doi:10.1016/j.sedgeo.2006.03.022

Weathering processes and, to some extent, the physico-chemical conditions during deposition may be constrained by using heavy minerals of different stabilities (De Jong and Van der Walls, 1971; Friis et al., 1980; Morton, 1984; Mange and Maurer, 1991; Dill, 1995). Numerous studies have dealt with the chemical stability of heavy minerals resulting in different orders of stability (Pettijohn, 1941; Nickel, 1973; Velbel, 1989). For a more detailed analysis by means of EMP (electronmicroprobe) members of the solid-solution series of amphibole, epidote, garnet and phosphates, which are of intermediate stability (Berner et al., 1980), are most useful.

Ultrastable minerals like Sn- or Ti oxides, tourmaline and zircon strongly resist chemical weathering and thus may be taken to normalize the quantity of labile constituents. As a consequence, the ZTR (zircon–tourmaline–rutile) maturity index was proposed by Hubert (1962). In the present investigation the stable and ultrastable minerals are not used for reference but as a shelter that may protect other heavy and light minerals of lesser resistance to chemical weathering, and thereby preserve the entire development of a placer formation. As melt inclusions, sheltered from outside influences within a magma on the ascent, could preserve a more original magma composition and tell the student something about the deeper parts of the earth interior, sheltered inclusions in debris of stream sediments are used as an archive that may tell the story of unroofing and help constrain the geomorphological and geological processes in a study area.

Cassiterite (SnO_2) and rutile (TiO_2), two tetragonal and isotype minerals, provide by their peculiar crystal habits and twinning laws (in German: "Visiergraupen") a positive effect on the infiltration and preservation of internal sediments in their mineral aggregates. Internal sediments and cement mineralization are common in calcareous sediments, but have not been studied this way in clastic sediments (Flügel, 1982). The assemblage of minerals, occluding or lining the interstices and washed into solution vugs may tell us a story about the processes operative in and around these trap sites of placers, beginning with the release of the sheltering mineral from its parent rock. Modern Sn–Ti oxide placers from an alluvial–fluvial drainage system that developed on the NE Bavarian Basement, Germany, were studied to get an idea on the supergene alteration in the depositional environment of the placers during the Late Mesozoic and Cenozoic. This method may also be applied to continental placer deposits elsewhere. Careful examination of terrigenous placers in Africa, SE Asia or central Europe may help retrace the weathering conditions of these synsedimentary deposits and used as an ore guide to the primary ore deposits (Raufuss, 1973; Aleva, 1985; Camm and Hosking, 1985; Yim, 1994; Fletcher and Loh, 1996; De Wit, 1999; Coakley and Mobbs, 2001; Corbett and Burrell, 2003).

2. Methods of investigation

The particle size of the clastic rocks under consideration was determined by sieving and by means of a sedigraph and the data obtained throughout these laboratory investigations were plotted in the conventional way as cumulative frequency curves using a mm scale along the *x*-axis. The quartiles Q_1 (25%), Q_2 (50%) and Q_3 (75%) formed the basis to calculate the Trask's parameters median grain size (Md) (Q_2) and sorting coefficient ($so=(Q_3/Q_1)^{1/2}$).

The heavy minerals (density > 2.9 g/cm^3) were extracted by means of Na-polywolframate. Petrographic studies involved examination of particulate sections, polished sections and X-ray diffraction analysis. The electron microprobe analysis was used to identify the chemical composition of mineral aggregates and the accessory minerals they contain. A total of 42 grains of nigrine and cassiterite have been investigated and 525 chemical analyses have been carried out by electron microprobe using a CAMECA SX100 equipped with five wavelength-dispersive spectrometers and a Princeton Gamma Tech energy-dispersive system. Oxide and silicate phases were analyzed at 20 kV acceleration voltage and 20 nA sample current (on brass). Counting times were 10 s on peak and 5 s on each background. Natural minerals and metals were used as standards. The following X-ray lines, spectrometer crystals and standards (in brackets) were used: Na Kα, TAP (albite); Mg Kα, TAP (chromite, kaersutite); Al Kα, (chromite, almandine); Si Kα (rhodonite, almandine); P Kα, PET (apatite); S Kα, PET (pentlandite); K Kα, PET (biotite); Ca Kα, PET (apatite, kaersutite); Sc Kα, PET (metal); Ti Kα (rutile, kaersutite); V Kα, LIF (metal); Cr Kα, LIF (chromite); Mn Kα, LIF (rhodonite); Fe Kα, LLIF (magnetite, almandine); Ni Kα, LLIF (metal); As Lα, TAP (AsGa); Nb Lα, PET (metal); Sn Lα, PET (metal); Ta Lα, LIF (metal); W Lα, LIF (metal); Pb Mα, PET (PbS); U Mα, PET (metal).

3. Geological setting

The study area lies in the crystalline basement, covering part of the Moldanubian Zone at the western edge of the Bohemian Massif (Franke, 1989). A more

detailed picture of the lithology in the immediate surroundings of the drainage system has been drawn by Forster (1965) (Fig. 1). The major part of the study area is underlain by Precambrian paragneisses, composed of variable amounts of biotite, sillimanite, cordierite, quartz, garnet, and feldspar intercalated with some calcsilicate gneisses and amphibolites. Second in abundance are igneous rocks of Late Carboniferous age gabbroic to granitic in composition. In the wake of the granitic intrusions, acidic differentiates evolved, including aplites and pegmatites very much different in their mineral compositions. Some of these are strongly enriched in Nb oxides and Li–Mn phosphates (Strunz et al., 1975). Swarms of quartz veins bound the Late Variscan granite province towards the west (Fig. 1). After the Variscan orogeny, the NE Bavarian Basement was subjected to a strong uplift only interrupted by marine transgressions that encroached upon the basement at its western edge. Detritus eroded during uplift accumulated in various terrigenous depositional systems along the western edge of the basement in the south German Basin, as proved by heavy-mineral analyses of foreland sands (Schnitzer, 1957; Tillmanns, 1978; Salger, 1985; Dill, 1989, 1995). In the basement, proper, clastic sediments and relics of the Cenozoic regolith were, locally, preserved on a low-relief landscape. These relic landforms date back to the Late Mesozoic and the Early Cenozoic when subtropical climates dominated what is today the "Oberpfaelzer Wald" (Louis, 1984; Borger et al., 1993). By the end of the last glaciation, channels of the present fluvial systems incised into the basement rocks and transported debris of the older regolith and lithoclasts eroded during the glacial period.

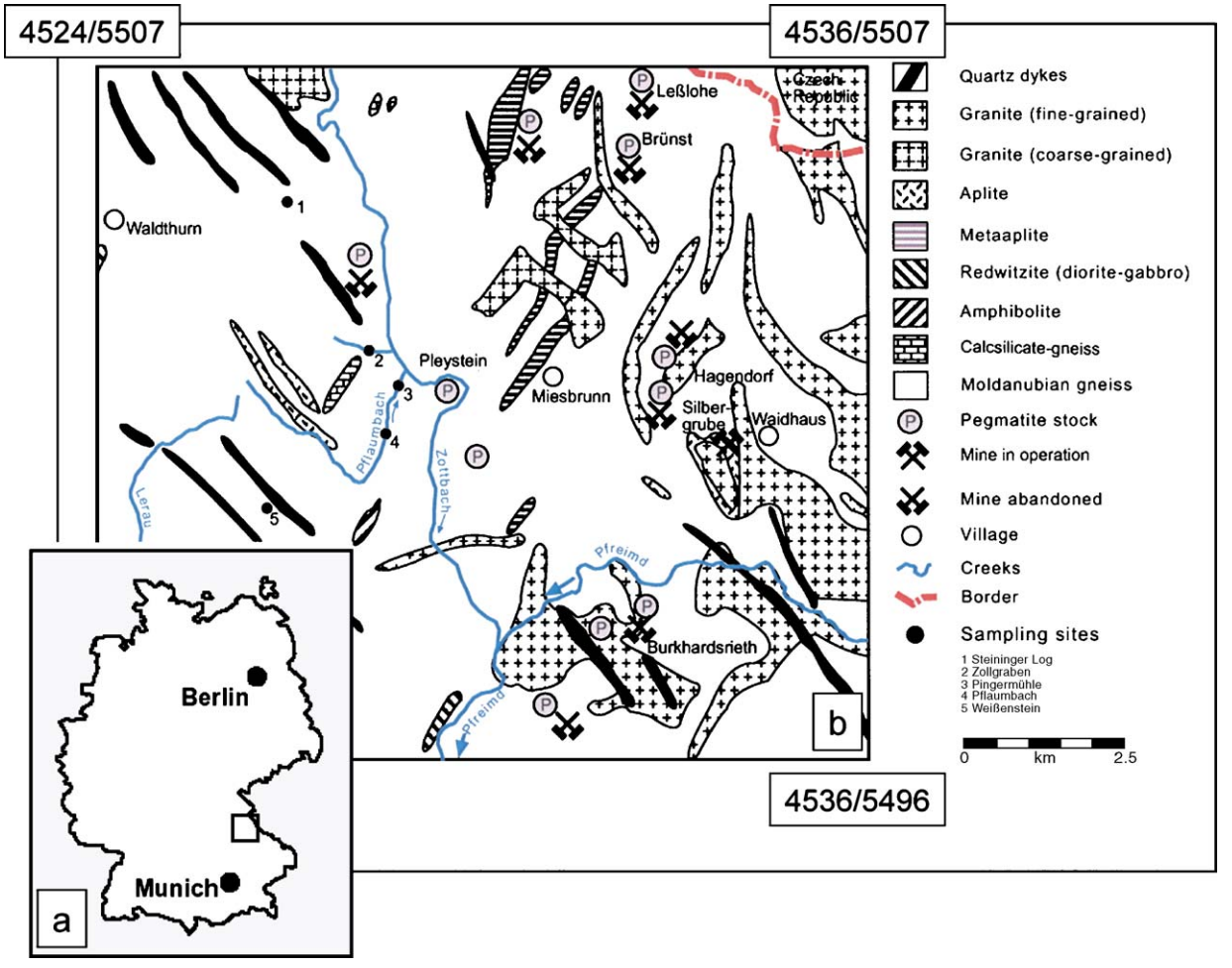

Fig. 1. Position of the study area in Germany (a). Sketch map to show the regional geology in the area around Pleystein NE Bavaria, Germany (modified after Forster, 1965) (b). Sampling sites considered throughout this study are shown by arabic numerals.

4. Results

4.1. Lithology and distribution of Sn–Ti placer deposits

Placer deposits are widespread in the fluvial drainage system around Pleystein (Fig. 1). The trap sites of these heavy minerals are in creeks that drain the western and northwestern slopes of a bowl-shaped depression with the quartz-pegmatite stock of Pleystein at its center. Outside this depression, concentrations of Ti- and Sn minerals are absent in stream sediments, but were sporadically found embedded in quartz veins striking in NW–SE orientation (Figs. 1 and 2).

In the present-day channels, the Ti- and Sn placer minerals are scattered between poorly sorted gravels of vein quartz and clasts of metamorphic rocks (Fig. 3a). Mostly clast-supported, but locally matrix-filled, massive to crudely imbricated pebbles and gravels form a veneer that rests on top of the crystalline basement or infills bedrock crevices in the channels. It is a single-channel drainage system of low-sinuosity-type sensu Winterbottom (2000), with active channels measuring as much as 1 m wide and 0.5 m deep. Grassland covers the gently dipping slopes of the valleys along the lower reaches and coniferous trees in the headwaters extend over several tens of meters on both sides of the channel.

In a longitudinal section from the head waters to the river mouth, no regular variation of placer minerals is recognized: patchy heavy-mineral accumulations measure a few meters in length, with sharply bounded upstream and downstream ends.

Cassiterite grains mainly fall in the narrow range of 1.6 to 3.2 mm, whereas Ti minerals associated with cassiterite cover a wider grain-size spectrum. The maximum grain size of ilmenite–rutile aggregates exceeds 1 cm and the minimum grain size lies well below 0.1 mm (Fig. 4). The sorting of the arenaceous placer deposits is rather good with sorting coefficients in the range 1.2 to 1.6 (Fig. 5). The coarse-grained channel lag deposits in which Ti and Sn minerals reach a maximum are poorly sorted.

The placer minerals differ widely in grain shape, the majority being poorly rounded sensu Illenberger (1991). Crystal aggregates show beveled edges, chatter marks, and fretted surfaces (Fig. 3b).

4.2. Mineralogy of oxide minerals in Sn–Ti placer deposits

4.2.1. Cassiterite

Cassiterite forms a wide range of complex aggregates made up mainly of anhedral grains. Towards the edge

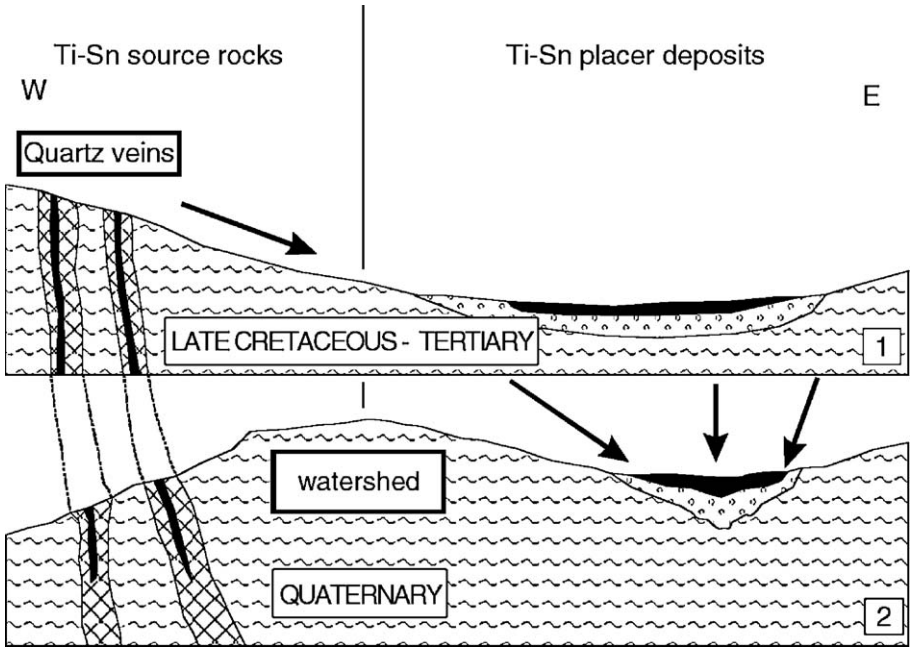

Fig. 2. Cartoon to show the evolution of placer deposits in relation to a potential source rock in the Pleystein area in NE Bavaria, Germany. (1) Evolution of the palaeoplacer during the Late Cretaceous and Early Tertiary (stages II to IV). Debris was delivered by the erosion of quartz veins at the western edge of the Hagendorf pegmatite province (stage I). (2) Evolution of the modern placer (stages V and VI) in the Pleystein area. For more explanation about the stages see Table 1.

Fig. 3. Distribution and morphology of placer minerals. (a) Bed load deposits of subrounded grains of placer minerals disseminated between gravel of vein quartz (bright) and gneiss (dark gray) in a creek near Pleystein. (b) Crystal aggregates of nigrine showing beveled edges. (c) Panned angular to rounded grains of monazite from the creeks around Pleystein.

the intimate intergrowth of anhedral grains alters into more stubby subhedral crystals. This transitional zone is characterized by numerous hexagonal voids filled with a wide variety of minerals (Tables 1 and 2) (Fig. 6a). The interelement relationships of Ta, Nb, V, Fe, and Mn in cassiterite are crucial to determine its temperatures of formation (Möller et al., 1988). Our investigation reveals that the cassiterite clusters are almost chemically pure SnO_2 with low concentration of FeO (<0.14 wt.%) and Nb_2O_5 (<0.5 wt.%), with Ta, V, Mn and W below the detection but TiO_2 from 0.4 to 0.8 wt. (Table 2). Accessory minerals that fill the hexagonal interstices, fissures, or are included in the cassiterite grains are the only impurities identified under reflected light and by EMP analysis in the cassiterite grains from the Pleystein area, Germany (Fig. 6b).

4.2.2. Titanium dioxides

The most common minerals in the cassiterite clusters are modifications of Ti dioxide, which are distinct in their trace elements and siting. Small slender grains up to 100 μm long form inclusions in cassiterite. They are strongly enriched in Fe, W, and Nb (Table 2). Some Nb-enriched rutile occurs as lamellar inclusions in nigrine aggregates (Nb_2O_5 1.6 to 18.5 wt.%, WO_3<1.2 wt.%, FeO 0.7 to 5.6 wt.%). The same sort of Ti oxide is found together with cassiterite in the placer deposits (Table 3, Fig. 6c). The black ferruginous rutile, locally intergrown with ilmenite in a wide range of textures was called nigrine by Ramdohr (1975), a term that sparked a lot of debate (Fig. 6c). The name ilmenorutile is used synonymously to describe Ti–Fe aggregates in cassiterite (Ramdohr,

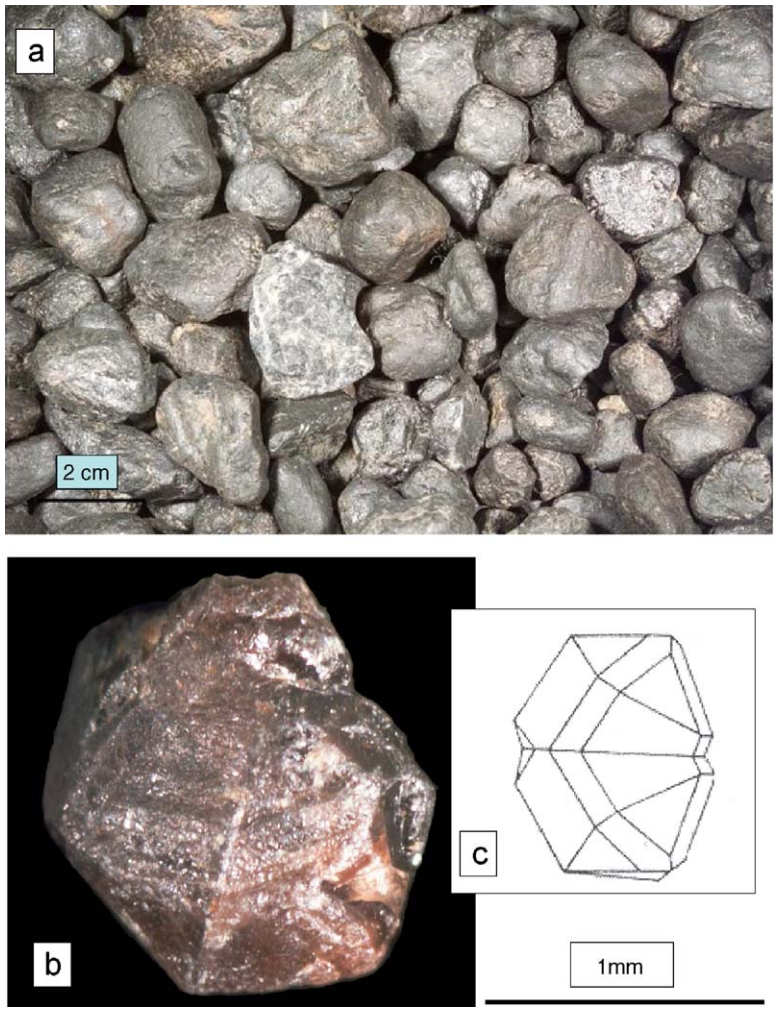

Fig. 4. Grains of cassiterite and nigrine from the colluvial–fluvial placers near Pleystein. (a) Subrounded to rounded grains of nigrine concentrated manually by panning in the field. Location near Pleystein. (b) Subrounded cassiterite aggregate made up of twinned cassiterite crystals. (c) Idealized intergrowth of twinned cassiterite crystals.

1975). There are zoned grains where ilmenite forms the rim or trellis-like exsolution lamellae (Table 3, Fig. 6c). Inclusions of rutile in the cassiterite from Pleystein were called niobian rutile due to the elevated content of Nb, following the proposal by Èerny et al. (1999). Besides nigrine and niobian rutile, another modification of Ti oxide lines the voids in cassiterite (Fig. 7). This type of Ti oxide lacks minor elements. Also the Nb contents are much higher in the cassiterite than in the void-filling Ti oxide. This cavity TiO_2 is interpreted as anatase, although the presence of brookite cannot be ruled out. X-ray diffraction analyses to discriminate anatase and brookite failed due to the tiny grain size. Raman spectroscopy would be the method to solve this problem.

4.2.3. Ilmenite

Ilmenite is third in abundance among the oxide minerals of the placer deposits. It is intergrown with niobian rutile leading to the nigrine aggregates mentioned above. Ilmenite also is a rare inclusion in cassiterite. It may contain elevated Mn contents, which are homogeneously admixed to the ilmenite solid-solution series. Only in one grain of nigrine does the pyrophanite component reach 8% to 9% and the solid-solution series may thus be termed manganiferous ilmenite.

4.2.4. Columbite

Columbite is a rare mineral also included in cassiterite and in rutile. Based on major elements, the

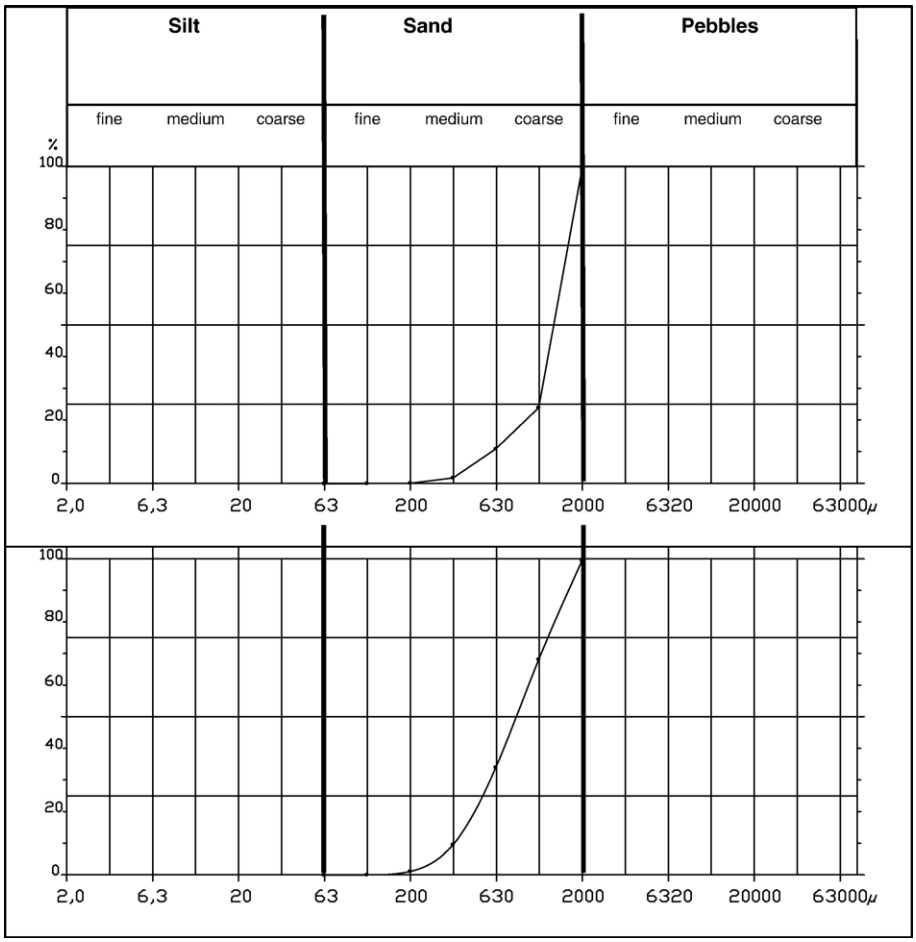

Fig. 5. Cumulative grain size curves of arenaceous Sn–Ti placers in the creeks around Pleystein, Germany.

Nb-bearing oxide is ferrocolumbite. Manganese, tantalum and tungsten are minor constituents (Table 2).

4.2.5. Quartz

Quartz is sporadically found in cassiterite, and is a ubiquitous gangue mineral in the placer deposits.

4.3. Mineralogy of oxide–hydroxide minerals in Sn–Ti placer deposits

4.3.1. Pseudorutile

Pseudorutile is a common mineral which replaces ilmenite along the edges and fissures in all types of nigrine. It forms small plates up to 20 μm in length and 2 μm in width closely associated with aluminum–phosphate minerals (see next chapter) in the internal sediments filling vugs in the cassiterite under study. Ti/(Ti+Fe) ratios are between 0.5 and 0.63 and may overlap with Ti/(Ti+Fe) ratios of ilmenite between 0.5 and 0.55. By definition, Ti/(Ti+Fe) ratios between 0.6 and 0.7 qualify Ti–Fe compounds as pseudorutile, while minerals with lower ratios are rather called hydroilmenite (Frost et al., 1983). Most of the alteration zones around or dendritic alteration zones within ilmenite grains are called hydroilmenite grading imperceptibly into pseudorutile.

4.3.2. Leucoxene

Leucoxene is not very much different from pseudorutile as to the environment of formation. It differs from other Ti-oxide compounds observed in the cassiterite clusters predominantly by its elevated Ti/(Ti+Fe) ratios exceeding 0.7.

4.4. Mineralogy of aluminum–sulphate–phosphate minerals (APS) in Sn–Ti placer deposits

APS minerals occur in a wide range of environments of formation covering the metamorphic, igneous and sedimentary realms (Dill, 2001). The minerals have the

Table 1
Source rock and placer evolution in the NE Bavarian basement around Pleystein with an appendix to show the names and formulas of all minerals used in the text and in the tables

Provenance analysis	Environmental analysis				
Stage I	Stage II	Stage III	Stage IV	Stage V	Stage VI
Inclusions	Host	Fissure filling	Cavity lining	Cavity filling	Colluvial–fluvial sediments
Pegmatitic–hydrothermal granitic stage	Peneplanation and deposition of paleoplacers in shallow valleys	Chemical weathering and replacement of preexisting Fe-bearing oxides and phosphates	Neomorphism of alteration minerals	Internal sedimentation	Deposition of modern placers
Physico-chemical conditions: $T \pm 450$ °C, pH > 7, Eh ≈ 0	Physico-chemical conditions: $T > 22$ °C, pH < 7, Eh > 0	Physico-chemical conditions: $T < 50$ °C, pH 4–6, Eh > 0	Physico-chemical conditions: pH < than in stage IV	Physico-chemical conditions: pH ≥ 7, Eh ≤ 0	Physico-chemical conditions: pH ± 7, Eh > 0
Age of formation: Carboniferous–Permian	Age of formation: Late Cretaceous to Tertiary	Age of formation: Late Cretaceous to Early Tertiary	Age of formation: Late Cretaceous to Early Tertiary	Age of formation: Late Tertiary to Quaternary	Age of formation: Quaternary
Ferrocolumbite					
Manganiferous ilmenite					
Niobian rutile					
Cassiterite	Cassiterite				
	Nigrine				
		Pseudorutile–leucoxene			
		Gorceixite–florencite s.s.s.	Gorceixite–florencite s.s.s.		
		Gorceixite–florencite–plumbogummite–crandallite–s.s.s	*Gorceixite–florencite–plumbogummite–crandallite–s.s.s*		
			Unidentified Fe–Al phosphate or intergrowth of strengite and variscite (?)		
			Anatase	Pyrophyllite (?)	
			Kaolinite	Kaolinite	
				Kaolinite–illite mixed-layer	
				Ca-Smectite	
				Quartz	Quartz
				Alkaline feldspar (albite)	Alkaline feldspar
				Epidote (pistacite)	

Muscovite–phengite	Muscovite
Biotite	
Chlorite	Chlorite
Ilmenite	
	Amphibole
	Vermiculite
	Monazite

In the diagram to show the mineral assemblages as a function of time and variation of physicochemical conditions of the mineralizing fluids the major heavy minerals inherited from the crystalline source rocks, e.g. cassiterite, are shown in bold-faced characters, minerals of lesser abundance, such as Nb rutile included in cassiterite are written in normal characters and newly formed minerals such as gorceixite are given in italics.

Mineral	Formula
Alkaline feldspar (albite)	$NaAlSi_3O_8$
Amphibole	$Ca_2Mg_4Al_{0.75}Fe^{3+}_{0.25}(Si_7AlO_{22})(OH)_2$
Anatase	TiO_2
Biotite	$KMg_{2.5}Fe^{2+}_{0.5}AlSi_3O_{10}(OH)_{1.75}F_{0.25}$
Cassiterite	SnO_2
Chlorite	$Mg_{3.75}Fe^{2+}_{1.25}Si_3Al_2O_{10}(OH)_8$
Crandallite	$CaAl_3(PO_4)_2(OH)_5{\cdot}(H_2O)$
Epidote (pistazite)	$Ca_2Fe^{3+}_{2.25}Al_{0.75}(SiO_4)_3(OH)$
Ferrocolumbite	$(Fe, Mn)(Nb, Ta)_2O_6$
Florencite	$CeAl_3(PO_4)_2(OH)_6$
Gorceixite	$BaAl_3(PO_4)(PO_3OH)(OH)_6$
Ilmenite	$FeTiO_3$
Kaolinite	$Al_2Si_2O_5(OH)_4$
Leucoxene	Non-stoichiometric alteration product of various Ti minerals composed of Ti oxide
Monazite	$CePO_4$
Muscowite	$KAl_3Si_3O_{10}(OH)_{1.8}F_{0.2}$
Nigrine	Aggregates of ilmenite intimately intergrown with rutile
Plumbogummite	$PbAl_3(PO_4)_2(OH)_5{\cdot}(H_2O)$
Pseudorutile	$Fe^{3+}{}_2Ti_3O_9$
Pyrophyllite	$Al_2Si_4O_{10}(OH)_2$
Quartz	SiO_2
Rutile	TiO_2
Smectite	$Na_{0.2}Ca_{0.1}Al_2Si_4O_{10}(OH)_2(H_2O)_{10}$
Strengite	$Fe^{3+}(PO_4){\cdot}2(H_2O)$
Variscite	$Al(PO_4){\cdot}2(H_2O)$
Vermiculite	$Mg_{1.8}Fe^{2+}_{0.9}Al_{4.3}SiO_{10}(OH)_2{\cdot}4(H_2O)$

Table 2
Chemical composition of mineral inclusions and cavity fillings of cassiterite (data given in wt.%)

Mineral	Cassiterite	Cassiterite	Rutile	Rutile	Nb rutile	Ilmenite	Columbite	Columbite
Grain	2	2	6	6	2	6	2	2
Analysis	16	19	4	6	21	8	13	22
SnO_2	98.93	99.15	3.39	2.73	2.88	0.98	0.94	1.27
TiO_2	0.57	0.75	90.49	91.51	77.27	51.97	3.46	4.80
Nb_2O_5	0.50	0.05	2.64	2.41	13.86	0.33	70.76	70.10
Ta_2O_5	bdl	bdl	0.29	0.32	1.00	bdl	0.72	1.58
Al_2O_3	bdl	bdl	0.07	0.06	0.23	bdl	0.02	0.02
MgO	0.01	0.01	bdl	0.02	bdl	0.04	0.35	0.21
FeO	0.14	0.09	1.31	0.93	4.67	43.89	16.79	18.30
MnO	0.02	bdl	0.01	0.01	0.02	2.63	3.24	1.76
Sc_2O_3	bdl	bdl	bdl	bdl	bdl	bdl	0.12	0.06
V_2O_3	bdl	0.06	1.39	1.18	0.80	0.26	0.03	0.03
ZrO_2	bdl	bdl	0.03	0.03	bdl	0.06	0.32	0.31
WO_3	0.04	0.08	1.22	0.18	0.54	0.16	4.10	3.35
Total	100.48	100.34	100.95	99.56	101.47	100.39	100.93	101.82
Sn	0.980	0.982	0.037	0.030	0.033	0.020	0.084	0.112
Ti	0.011	0.014	1.866	1.895	1.653	1.973	0.582	0.797
Nb	0.006	0.001	0.033	0.030	0.178	0.008	7.144	6.997
Ta			0.002	0.002	0.008		0.044	0.095
Al			0.002	0.002	0.008		0.005	0.006
Mg	0.000	0.000		0.001		0.003	0.117	0.068
Fe	0.003	0.002	0.030	0.021	0.111	1.854	3.135	3.379
Mn	0.000		0.000	0.000	0.001	0.113	0.613	0.330
Sc							0.024	0.012
V		0.001	0.031	0.026	0.018	0.010	0.005	0.006
Zr			0.000	0.000	0.000	0.001	0.035	0.033
W	0.000	0.001	0.009	0.001	0.004	0.002	0.238	0.192
Cations	1.000	1.001	2.010	2.010	2.014	3.984	12.026	12.025
Oxygen pfu	2	2	4	4	4	6	24	24

"bdl" means below detection limit, "pfu" means per formula unit.

general formula $AB_3(XO_4)_2(OH)_6$, where A is a large cation (Na, U, K, Ag, NH_4, Pb, Ca, Ba, Sr, REE). B sites are occupied by cations of the elements Al, Fe, Cu and Zn. In nature, the anion $(XO_4)^{x-}$ is dominated by P and S. APS minerals occur as wall lining in vugs and in close association with Ti oxides as demonstrated by the chemical maps of Ti and P (Fig. 7). In the specimens under study Pb–Ca–Ba–Ce solid solution series of APS minerals form part of the pore filling between cassiterite crystals (Fig. 8a). Based upon the qualitative spectrum obtained from EMP analysis the mineral is interpreted in terms of a solid solution of gorceixite (Ba), florencite (REE) plumbogummite (Pb) and crandallite (Ca). In Fig. 8c a complex spectrum has been selected to show an APS solid solution series typical of APS minerals found in the cavities of cassiterite. Some fissures widening funnel-shaped to the edge of cassiterite also gave host to an APS mineral solid solution series with predominant florencite (Fig. 8b). Another complex Fe–Al phosphate, cannot be determined based on EMP analysis only. It might be cacoxenite $(Al,Fe^{3+})_{25}(OH)_{12}O_6(PO_4)_{17}\cdot 75H_2O$) or barrandite (Fe, Al) $PO_4\cdot 2H_2O$. An intimate intergrowth of strengite ($FePO_4\cdot 2H_2O$) and variscite ($AlPO_4\cdot 2H_2O$) may also plausibly explain the chemical composition.

4.5. Mineralogy of silicates in Sn–Ti placer deposits

Silicates were only observed in the cavities of the cassiterite aggregates (Fig. 7). This is conspicuously demonstrated by the Al, Fe and K distribution in the cassiterite aggregates (Fig. 7). Silicates have not been spotted as inclusions neither in the cassiterite nor in the nigrine aggregates.

4.5.1. Phyllosilicates

Kaolinitic clay minerals occur in two different modifications. One forms well-defined flakes of sheet silicates, the other is present in lumps. Illite is not very much different from kaolinite with respect to its grain and aggregate morphology. K, Mg and Fe present in these sheet-like aggregates and lumps are indicative of illite/muscovite. Calcium being present in the aggregates points to some mixed-layers with smectite.

Smectite occurs also as a phyllosilicate on its own. Small amounts of Fe–Mg chlorite and vermiculite are also present in the hexagonal voids in cassiterite. An unknown Si–Al phase was spotted in the EDS spectrum.

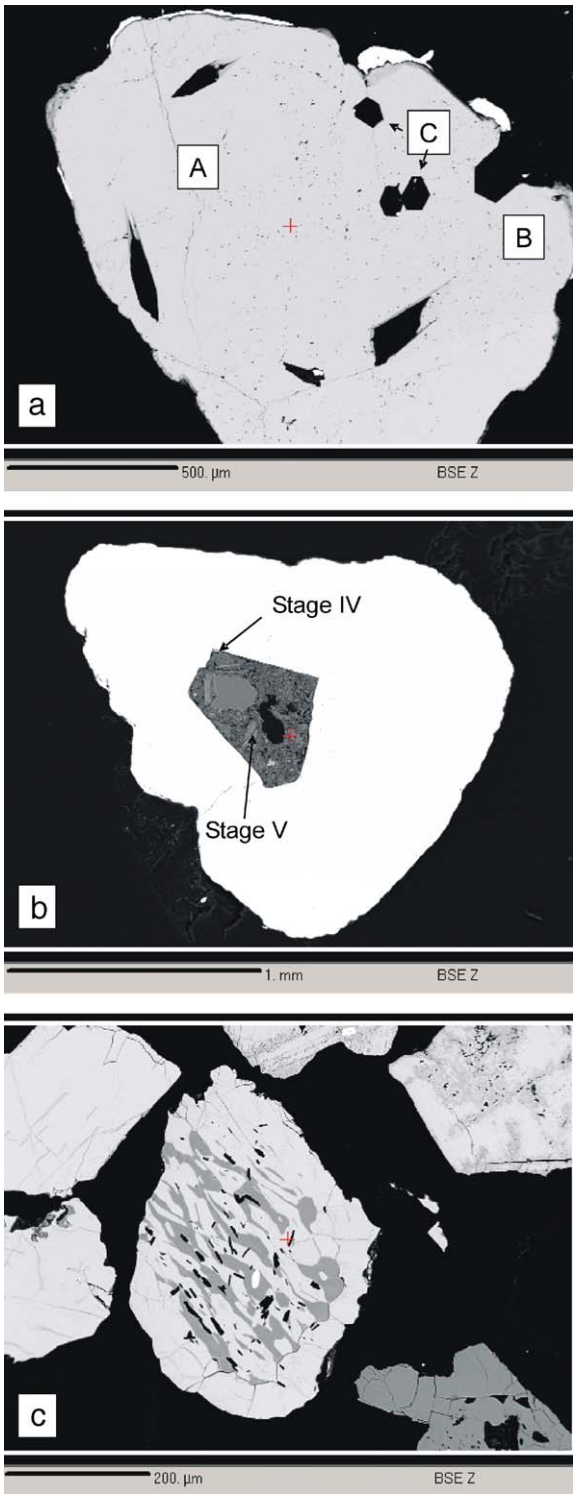

Its Al/Si ratio of 1:3 strongly contrasts with the Al/Si ratio of kaolinite (1:1) and illite (3:4). The ratio would well fit with pyrophyllite(?).

4.5.2. Framework silicates

Albite is present in angular grains.

4.5.3. Heavy minerals

Angular particles of epidote (pistazite) and amphibole were accumulated in the interstices of the cassiterite aggregates.

5. Discussion

5.1. Hypogene and supergene processes

The variability of accessory minerals in cassiterite aggregates from the Sn–Ti placer deposits allows for a subdivision of the entire placer mineralization into six stages covering the time span from the Late Carboniferous through the Recent. Stage I involves some kind of back-ward modelling, describing the potential source rocks that delivered the debris for the heavy mineral deposits. The environments of deposition and palaeo-weathering were discussed in stages II through VI of placer formation (Table 1).

5.2. Stage I—inclusions and provenance

Titanium minerals in the cassiterite aggregates under study offer a hint to the source rock of the debris in the placer. Several papers have addressed the petrological composition of recent sediments and the original source rocks, using Ti minerals as a link between source and depocentre (Basu and Molinaroli, 1989; Morton and Hallsworth, 1994; Alekseeva and Hounslow, 2004; Zack et al., 2002, 2004). The association of niobian rutile, Mn-bearing ilmenite and ferrocolumbite observed as mineral inclusions in cassiterite point to a pegmatitic

Fig. 6. Micrographs of cassiterite in the colluvial–fluvial placer (BSE/back-scattered-electron images). (a) Subangular cassiterite aggregate. Zone A consists of anhedral crystals of cassiterite—see gray seams marking the grain boundaries. Zone B is made up of stubby prismatic cassiterite crystals that are terminated by pyramids and zone C contains hexagonal voids. Irregularly shaped black dots scattered across the cassiterite cluster are mineral inclusions (stage I—see Table 1). (b) Subrounded cassiterite aggregate with a central void filled with minerals of stages IV and V denoted by the arrowheads. (c) A subangular aggregate of nigrine in the centre of the field of view shows an intimate intergrowth of ilmenite (bright) and rutile (dark). Other nigrine aggregates also to be seen in this BSE (back-scattered electron) image show different shades of gray that attest to pseudorutile and leucoxene both replacing the nigrine aggregates along cracks and at the edge.

Table 3
Chemical composition of nigrine types A, B and C associated with cassiterite in the placer deposits

Type	Nigrine type A	Nigrine type B 1	Nigrine type B 2	Rutile type C
Maximum size (mm)	11	6	6	0.5
Host	Rutile	Rutile/ilmenite	Ilmenite	Rutile
Lamellae in host		Nb-rutile	Nb-rutile	W-rutile
Rim	Ilmenite			
Lamellae in rim	Nb-rutile	Hematite		
Mineral inclusions in ilmenite	Wolframite, zircon, sphalerite, pyrrhotite	Columbite, pyrochlore, betafite, magnetite	Columbite, pyrochlore, wolframite, zircon	
Chemical composition (wt.%)				
Rutile host				
Nb_2O_5	0.1–1.4	0.3–0.4		0.15
FeO	0.2–0.7	0.4–0.8		0.5
Rutile lamellae				
Nb_2O_5	0.8–10.0	1.5–8.6	0–21	0.3
FeO	0.4–4.8	1.0–4.2	0–7	2
WO_3	0–2	0.6	0–2	5
Ilmenite				
Nb_2O_5	0.1–0.3	0.2	0.02–0.5	
MnO	1.1–4.0	2.4	1.5–9.0	

mineralization from which the cassiterite has been derived. Titanian ferrocolumbite was described by Èerny (1992) from beryl-bearing F-impoverished pegmatites. Columbites were also reported by Forster (1965) from the nearby pegmatite of the Hagendorf (56.5 wt.% Nb and 22.8 wt.% Ta). Another marker for a pegmatitic source rock is niobian rutile (Èerny et al., 1999). Cassiterite from Sn–W quartz veins in Portugal is unzoned, does not show any exsolutions and is poorer in Nb and Nb+Ta and richer in Ti than cassiterite from adjacent Li-bearing granitic pegmatite veins (Antunes et al., 2002). In conclusion, the accessory minerals in the cassiterite from the Pleystein area mark a pegmatitic source for the placer cassiterite mineralization. The source rock is supposed to be the quartz veins at the western edge of the Late Paleozoic Hagendorf pegmatite province (Fig. 1). The FeO contents of wolframite in granitic Sn–W-quartz veins in Portugal range from 16 to 17 wt.% FeO (Antunes et al., 2002). In the placer deposits the maximum content is much higher (24.28 wt.% FeO). Wolframite observed as tiny inclusions in some grains of nigrine might be correlated with the waning stages of the sulfide stage in the Hagendorf pegmatite which developed at approximately 450 °C (Mücke et al., 1990). Due to the high mobility of silica and the close association of oxidic minerals with minerals bearing iron in its bivalent state, the pH value was supposed to be greater than 7 and the Eh was fluctuating around 0 with conditions becoming more oxidizing towards younger stages in this granitic pegmatitic to hydrothermal source rock lithology.

Another argument for a pegmatitic–hydrothermal process in the source area is delivered by the crystal morphology of cassiterite which is locally well preserved in the placer aggregates.

Development of the crystal forms of minerals in space and time depends on the evolution of the mineral-forming environment, in other words physico-chemical parameters (temperature, pressure, supersaturation, pH). Cassiterite is an example of this crystallomorphological evolution of minerals, with bi-pyramidal crystals forming at the high-temperature end and slender crystals of needle tin and botryoidal wood tin occupying the opposite end of the temperature range. A micrographic documentation of this crystallomorphological sequence was presented by Dill (1985) for the cassiterite mineralization in NE Bavaria. The stubby crystals at the edge of the mineral aggregates (Fig. 6a), the overall pyramidal morphology (Fig. 6b) and the way crystal faces were terminating (Fig. 8b) the voids, rule out any derivation of the cassiterite grains in the placer from a source of low-temperature formation.

5.3. Stage II—host and peneplanation

Quartz veins which were identified as a potential source for cassiterite and for nigrine in stage I are separated today from the placer deposits in the creeks around Pleystein by a mountain ridge (Fig. 2). A bit of a curiosity, there is neither any accumulation of cassiterite nor of nigrine west of the present-day watershed, that is

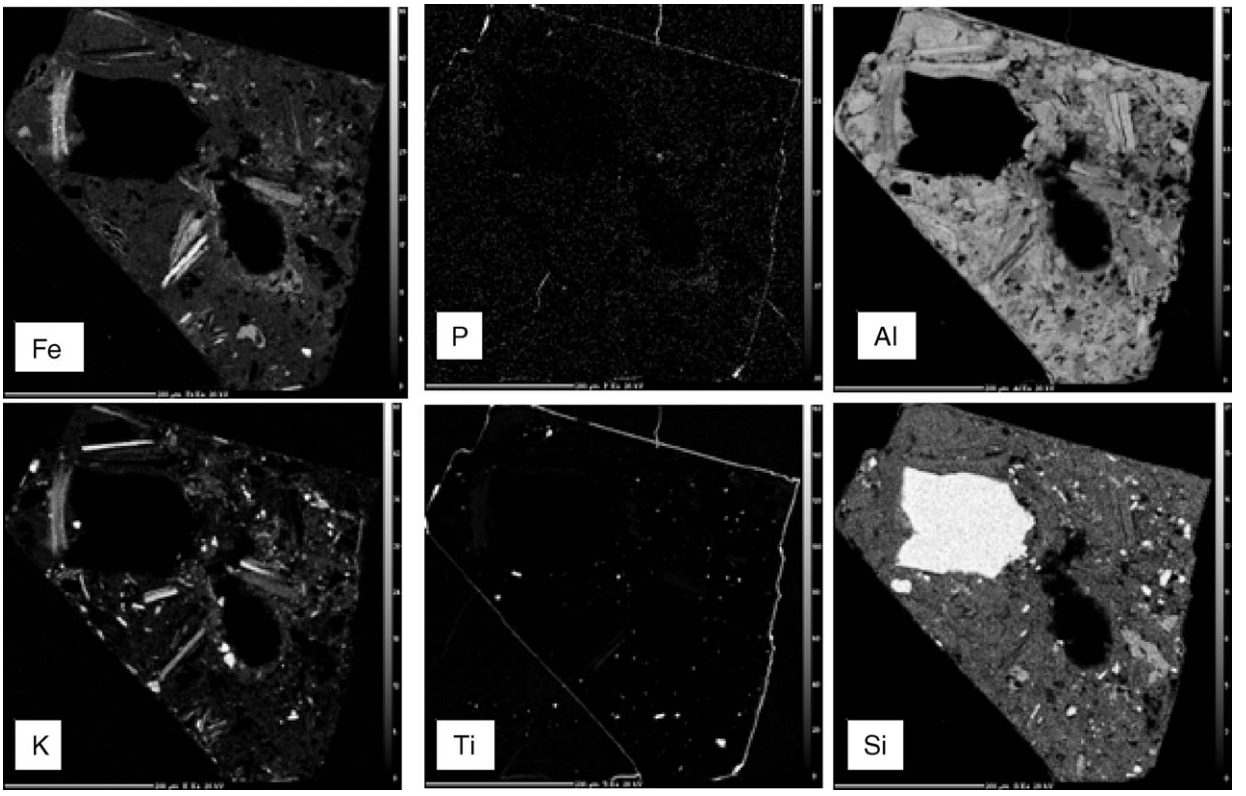

Fig. 7. Chemical maps of a void filling in a cassiterite aggregate of the colluvial–fluvial placer based on $Fe_{K\alpha}$, $P_{K\alpha}$, $Al_{K\alpha}$, $K_{K\alpha}$, $Ti_{K\alpha}$ and $Si_{K\alpha}$ radiation during EMP analysis.

the side of the quartz veins. When the Sn–Ti paleoplacers were formed, there was obviously no such divide between the Pleystein depocentre and the Ti–Sn source rocks so that nigrine and cassiterite grains could be transported unimpededly towards the east. The watershed or interfluve of the shallow valleys on the peneplain is likely to have been more westward than today. Since then, the quartz veins have been eroded down to a depth, where the intrinsic mineral content of the siliceous rocks can no longer act as a source for Ti and Sn in the creeks and rivulets draining the western slopes of the watershed (Fig. 2).

There is no regular increase in Ti and Sn minerals in the modern creeks towards the potential source area and thus the current accumulation of placer minerals in the creeks cannot be attributed entirely to the fluvial action of the recent drainage system. The catchment areas are very small, the grain size relatively large and the roundness very poor. Sheetwash and mass wasting processes on the valley slopes are more consistent with the observed size and morphology of grains in the placer deposits than pure fluvial transport under bedload conditions.

The palaeoplacer is supposed to have formed on a low-relief surface in a tropical wet–dry morphoclimatic zone, that sensu Tricart and Cailleux (1958) and Buedel (1977) is characterized by landforms called peneplains or etchplains. The evolution of such low-relief landscapes with shallow valleys, low terraces and gravel-topped interfluves was debated in various textbooks and comprehensive papers on geomorphology (Thomas, 1994; Twidale, 2002).

Under base level flow conditions (0.5 m^3/s) no bedload sediment is transported (Fletcher and Loh, 1996). After heavy rain storms flows rise rapidly to discharges that exceed 3.5 m^3/s. Bedload transport starts at a discharge of approximately 1.0 m^3/s and thereafter increases exponentially for all size fractions up to discharge of 2.2 m^3/s when the rate of sediment accumulation in the trap exceeds 5 kg/min. Such flow regimes occur under climatic conditions with strong contrasts during seasonal precipitation. They do not exist in the present-day fluvial drainage system.

Climatic conditions like those postulated for the deposition of the palaeoplacer during stage II in the NE Bavarian Basement exist today in tropical Africa.

Geomorphological processes resembling those in present-day tropical Africa, most favorable for (etch) planation, occurred during the Tertiary and the Late Cretaceous in what is called today the NE Bavarian Basement (Trusheim, 1936; Bremer, 1977; Buedel, 1977; Louis, 1984). Water temperatures exceeding 22 °C are very effective during chemical weathering, a prerequisite for the release of heavy minerals form their source rocks during peneplanation (Thomas, 1994).

Present-day peneplanation in tropical Africa is accompanied by pervasive chemical weathering leading to the formation of a thick regolith and to the decomposition of most of the light and heavy minerals except ultrastable compounds such as Ti- and Sn oxides. They were pre-concentrated in shallow depressions on the undulating peneplain/etch surface and at the lower edge of pediments (Fig. 2) (Dill et al., 2005). Not surprisingly, continental placer deposits of economic importance with predominantly ilmenite and rutile are very widespread in central Africa, e.g. Malawi: Heavy mineral sands at Salima-Chipoka are placed at 700 Mt, grading an average of 5.6% heavy mineral and at Mangochi at 800 Mt, grading an average of 6.0% heavy mineral (Ministry of Energy and Mining, 1997; Coakley and Mobbs, 2001).

The pH values of the meteoric fluids during stage II of placer formation was well below 7 otherwise minerals of lesser stability would have been preserved under these conditions. All heavy minerals occur as liberated grains unlocked from quartz which was decomposed under the tropical (palaeo)climatic conditions.

5.4. Stage III—fissure filling and replacement of preexisting minerals

Open fissures in cassiterite were sealed with various APS minerals and ilmenite included in cassiterite was replaced at the edge by boxwork pseudorutile and by leucoxene which evolves during an advanced stage of weathering at the expense of pseudorutile. Despite the refractory nature of Ti, studies have documented Ti mobility in soils and sediments (Gardner, 1980). Laboratory and field studies suggest that organic acids and CO_2-rich groundwaters can solubilize Ti (AlDahan and Morad, 1988). Mücke and Bhadra Chaudhuri (1991) showed that the alteration of ilmenite by leaching is a continuous process, proceeding from "leached ilmenite" through pseudorutile to leucoxene. In this process which takes place near the surface the presence of water is required and temperature does not exceeded 50 °C. Diffusion processes are of no importance in this mineral transformation.

Phosphate minerals as they were identified in the cassiterite aggregates are crucial for a palaeohydrological and environmental interpretation. Apatite and aluminum phosphate solid solutions are very sensitive to changes in the acidity of the pore fluids. Primary phosphates such as apatite are entirely absent in the mineralization under study. This has some implications for the change of the pH values of the meteoric waters coming into contact with the various heavy minerals. According to the experimental data of Nickel (1973)

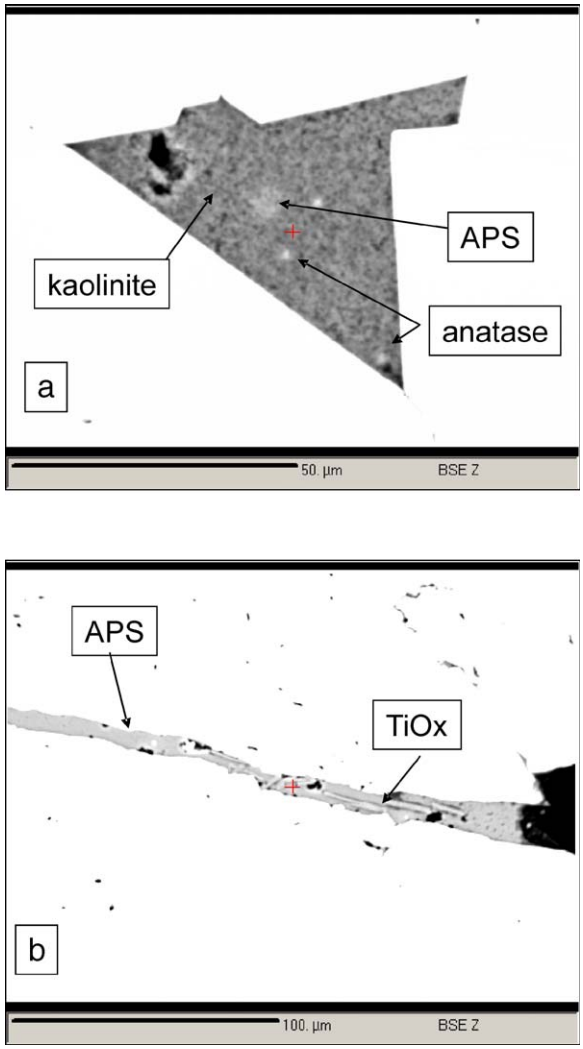

Fig. 8. Micrographs of aluminum phosphates (APS) in cassiterite (BSE images). (a) Cavity in a cassiterite cluster filled with aluminum phosphates (APS) composed of gorceixite (Ba), florencite (REE/Ce), plumbogummite (Pb) and crandallite (Ca). (b) Fissure filled with aluminum phosphates (APS) enriched in florencite. The aluminum phosphates is associated with pseudorutile (TiOx) c) EDS (energy-dispersive) spectrum of aluminum phosphates (see a). The $Si_{K\alpha}$ peak is attributed to quartz.

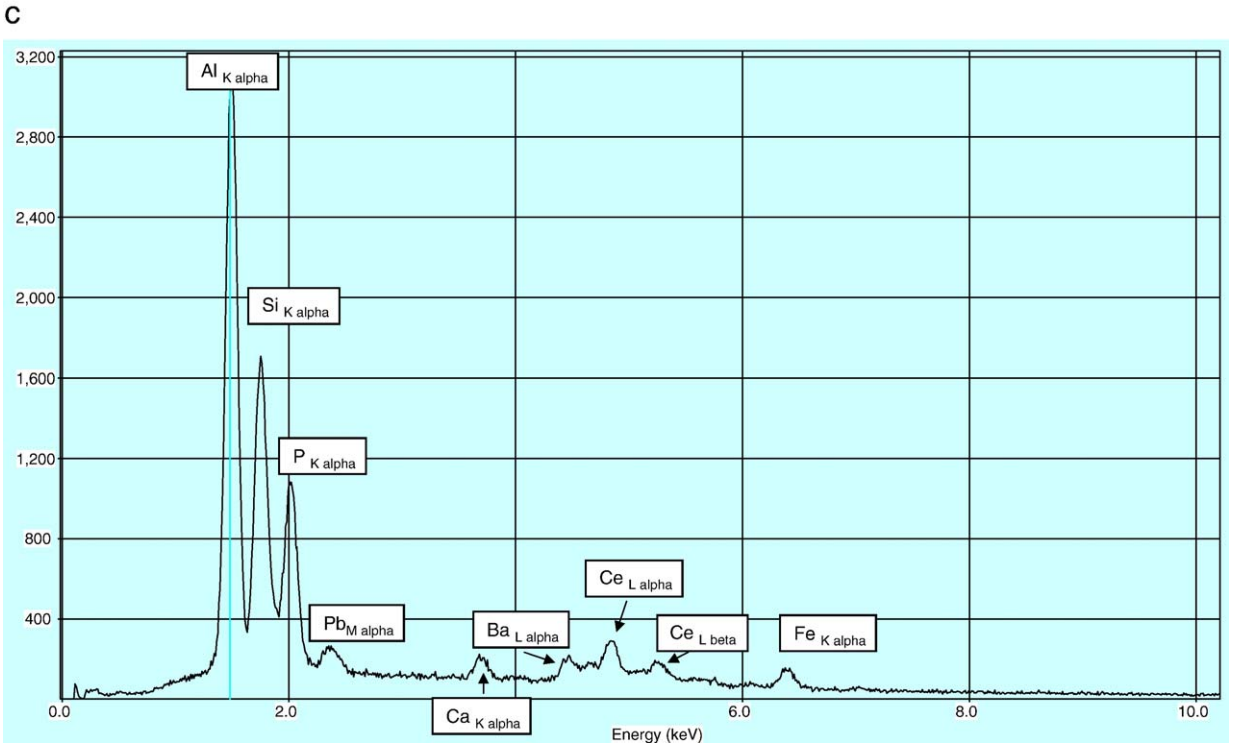

Fig. 8 (*continued*).

apatite dissolution is very rapid in groundwater of pH < 5.6 and APS minerals form instead. Only minerals of the APS solid solution series, the most common representative of which is given in the equation below, are stable under acidic porewater conditions. CO_2-rich waters, as expected for the dissolution of primary Ti minerals, were also responsible for the elimination of primary phosphates which are much more susceptible to acidification of the meteoric waters than primary Ti oxides.

$$\text{apatite} + 3Al(OH)_4 + 9H^+ \Rightarrow \text{crandallite} + 4Ca^{2+} + HPO_4^{2+} + 7H_2O.$$

Barium and lead in the unit cell of APS minerals have been derived from the decomposition of alkaline feldspar, where Ba and Pb may substitute for K^+. Calcium has been derived from the decomposition of apatite and plagioclase, both of which are very much susceptible to weathering. Rare earth elements necessary for the built-up of florencite originated from monazite and xenotime, both of which may be traced back to the late Variscan granites nearby. These REE minerals were not encountered as inclusions in cassiterite. Single crystals of monazite, however, may be found in the stream sediments of the creeks—see stage VI (Fig. 3c). Another source for REE may be pyrochlore that was locally spotted in nigrine aggregates.

At high H_3PO_4 concentrations apatite is stable down to a pH of about 6. In this case crandallite appears first among the APS minerals. Increasing acidity of the pore solution and a lowering of the pH value down to 4 causes augelite ($Al_2(PO_4)(OH)_3$) or wavellite ($Al_3(PO_4)_2(OH)_3F_{0.5}\cdot 5(H_2O)$) to come into existence depending on the quantity of H_3PO_4 (log a $H_3PO_4 = -2.75$). At a very low quantity of H_3PO_4 (e.g. log a $H_3PO_4 = -9$) apatite at a pH value of approx. 7 is converted into woodhouseite ($CaAl_3(PO_4)(SO_4)(OH)_6$). Ongoing lowering of H_3PO_4 will lead to gibbsite as the final product of phosphate alteration. Neither gibbsite nor the sulfate-bearing analogues of the crandallite solid solutions series are present in stage III mineralization. Therefore pH conditions in the range 4 through 6 are supposed to have occurred during stage III of placer formation.

Elevated Pb contents were recorded from several kaolinitic saprolites in Germany as old as Triassic. A relative "high" of Pb enrichment in kaolin was established for the Late Cretaceous and Early Tertiary (Störr, 1975; Störr et al., 1991). The anomalously high Pb contents are caused by plumbogummite present in

the kaolinitic host rocks. Gorceixite- and florencite-specialized APS mineralizations were also reported by Dill et al. (1995) from Tertiary kaolinitic saprolite in the Rheinisches Schiefergebirge, Germany. Modifiers such as AsO_4^{3-}, CO_3^{2-} and SiO_4^{2-} can proxy for the $(XO_4)^{x-}$ anion complex in APS minerals contained in kaolinitic saprolite (Hak et al., 1969).

Even if no precise age determination can be achieved by this mineralogical correlation ("minero-stratigraphy") of APS minerals in cassiterite with APS mineralization elsewhere in Central Europe, a Late Cretaceous to Early Tertiary age of formation is likely for the mineralization of stage III. Further support to this idea is provided by analyses of clay minerals of sediments in NE Bavaria carried out previously by the senior author. They revealed that the content of kaolinite may reach as much as 90% in samples of Early Tertiary age. During the Late Tertiary, kaolin contents rapidly go down to as much as 35% in samples from the study area in NE Bavaria.

5.5. Stage IV—cavity lining and neomorphism

Ilmenite alters to microcrystalline anatase via pseudorutile (Anand and Gilkes, 1984), but other mafic minerals such as amphibole and biotite may also act as source for Ti in anatase. In stage III, primary Ti minerals (ilmenite) and secondary Ti minerals (pseudorutile) are intimately intergrown with each other. In stage IV, source mineral and replacement product are apart from each other and no longer related in space. Ti polymorphs such as anatase and brookite, kaolinite and APS minerals are lining the cavities in cassiterite aggregates with no direct contact to any precursor Ti material. As far as the APS minerals are concerned, there is little compositional difference between stage III and stage IV. In addition to the APS minerals reported from stage III, there is only one Fe–Al phosphate which cannot be determined precisely without XRD. Anatase and kaolinite are confined to open-hole fillings and wall linings of hexagonal cavities which are predominantly favored by the complex twinning laws of cassiterite (Fig. 4c). Cassiterite belongs to the tetragonal–ditetragonal dipyramidal crystal system and forms often doubly terminated crystals. This peculiar crystallographic habit and the twinning law are responsible for the well-shaped voids shown in Fig. 6a and in a cartoon in Fig. 4c.

No gibbsite–alunite association has been observed in the cavities.

$$3AlO(OH) + (K,Na)^+ + 3H^+ + 2SO_4^{2-} \Leftrightarrow (K,Na)Al_3(SO_4)_2(OH)_6$$

Only kaolinite is related in space and time with APS minerals

$$2Al_2Si_2O_5(OH)_4 + 2(Na/K^+) + 6H^+ + 4SO_4^{2-} + 9H_2O \Leftrightarrow 2(K,Na)Al_3(SO_4)_2(OH)_6 + 6H_4SiO_4(aq)$$

Kaolinite is one of the clay minerals, playing a decisive role in removing REE from aqueous solutions as has been demonstrated by laboratory experiments (Aja, 1998). Kaolinite in surface weathering systems scavenges significant amounts of REE from aqueous solutions (Putter et al., 2002). Not surprisingly, coatings of kaolinite may be found in the cavity fillings also containing significant amounts of florencite. The phase boundary between strengite, that may best represent the unidentified Fe–Al phosphate of stage IV, and goethite is negatively skewed in the log $a_{HPO_4}^{2-}$ vs. pH diagram, running between 4 and 5.8. Therefore the mineral association described as Fe-bearing APS minerals, anatase and kaolinite "in" and goethite "out" reflects a moderate lowering of the pH relative to stage III (Dill et al., 1991).

5.6. Stage V—cavity filling and internal sedimentation

The internal sediments deposited in the cavities of cassiterite aggregates during stage V are very heterogeneous, pointing to conflicting physico-chemical conditions if they were held to be contemporaneous in origin. Ilmenite has already been mentioned as a marker mineral indicative of the source rock environment (stage I) and kaolinite as some kind of a geo-acidometre (stage IV). Besides kaolinite and kaolinite–illite mixed layers, smectite appears among the sheet silicates of stage V. Smectite forms in alkaline environments (Howard and Fisk, 1988). Formation of kaolinite, on the other hand, occurs in acidic conditions (Huertas et al., 1999) if the (alkali)/(H^+) ratio is low (Eberl and Hower, 1975). There are phyllosilicates bearing bivalent Fe such as chlorite and biotite, which can only be preserved under moderately oxidizing conditions and heavy minerals like epidote/pistazite which also are known to be of moderate resistance to weathering. The internal sediments in cassiterite are compositionally very immature and were delivered from different sources. Phyllosilicate assemblages with prevailing kaolinite are interpreted as reworked regolith of Early Tertiary age (see previous stages). Smectite and heavy minerals of lesser resistance to weathering reflect more alkaline pore solutions and post-date kaolinization in the study area. They are typical of planation processes

operative during the Late Tertiary (Sarmatian–Pontian) in NE Bavaria (Louis, 1984). Sheet silicates containing bivalent Fe can only be preserved under poorly aerated conditions as are the case in sealed cavities or in waterlogged deposits. Stage V is representative of the modern placer deposits. It encompasses relics of an intermediate stage of (etch)planation of the NE Bavarian Basement during the Late Tertiary mixed up with minerals provided by the mechanical weathering during the glacial period.

5.7. Stage VI—colluvial–fluvial deposition of modern placers

A set of minerals neither found occluding the pore space nor being included by cassiterite are closely related with cassiterite in the modern creeks. They have been listed in a stage of their own. This mineral association is made up predominantly of labile constituents and reflects present-day weathering conditions.

Patchy heavy mineral accumulations around Pleystein got their final shaping by periglacial solifluction. Subsequently, small creeks incised into these solifluction terracettes and reworked the Sn- and Ti-bearing debris. The transport regime along the slopes is characterized by mass flows that pass upslope into solifluction/gelifluction sheets and soil creep. Towards the thalweg, mass flows grade into coarse-grained gravel deposition of low-sinuosity fluvial streams. The lack of internal structures in the bedsets, missing cross-cutting bedforms, channels or scouring and a coarsening-upward trend in the grain sizes suggest deposition as a combination of fluvial bedload and colluvial slope processes (Smith, 1992; Washburn, 1981; French and Guglielmin, 1999). Fluvial reworking was of lesser intensity than the slope processes, otherwise these patches of heavy minerals would have been largely dispersed downstream in the modern drainage system.

Poor roundness of clasts is a direct response to the very short distance of transport. On the other hand, the short distance of transport could not have given rise to a rather well-sorted sediment. The very homogeneous particle size, especially in the placer deposits, reflects the original size during crystallization in the source–see stage I–rather than abrasion during transport. Locally, the crystal shape of the cassiterite is still well preserved —see stage I (Fig. 3) (Yim, 1994).

6. Conclusions

The Sn–Ti placer deposits found in creeks incised into basement rocks and their semi-consolidated overburden around Pleystein, Germany, may be categorized as colluvial (to fluvial) in origin. According to the characteristics–small size, developing on an erosional surface–summarized by Stanaway (1992), the placer deposits may be called trap placers rather than bed placers. The stanniferous trap placer arose from reworking of a low-grade bed placer (see below).

The placer deposits originated from a pegmatitic–hydrothermal source of Late Variscan age whose physico-chemical conditions may be constrained by careful examination of the cassiterite aggregates (stage I). This is based on mineral inclusions in cassiterite containing Ti and Nb and on morphological grounds. During the Late Cretaceous and early Tertiary a palaeoplacer developed in the study area in an environment resembling the savanna or peneplains in tropical Africa (stages II–IV). Uplift and denudation of the NE Bavarian Basement gave rise to a polycyclic evolution of the landscape with (etch)planation being the most efficacious geomorphological process during the Cenozoic in this area. A rapid increase in the rate of uplift during the Quaternary triggered the incision of rivers into the basement and brought deposition of Sn–Ti placers to a halt. The modern placers (stages V–VI) are representative of the waning stages of placer formation and held to be relic deposits which are only moderate economic value due to the limited size.

The technical approach can be used for the delineation of continental placers elsewhere and as an ore guide to primary Sn deposits or sites mineralized with pegmatites that otherwise are difficult to explore for their lack in heavy minerals resistant to weathering and attrition during transport. Such a target area where these data may be of assistance for exploration is located in Central African savanna where heavy mineral sands were deposited along the western shoreline of Lake Malawi and in the nearby drainage systems cutting upstream into crystalline bedrocks intruded by pegmatites (Coakley and Mobbs, 2001).

Acknowledgments

We are indebted to J. Lodziak who conducted the microprobe analyses and I. Bitz for her assistance during the separation of heavy minerals and grain size analysis. We express our gratitude to K.A.W. Crook for editorial handling of the submitted paper and his comments to a previous draft. We extend our gratitude also to three anonymous reviewers who took over the task of reviewing the paper for SEDIMENTARY GEOLOGY and made helpful comments to the manuscript.

References

Aja, S.U., 1998. The sorption of the rare earth element, Nd, onto kaolinite at 25 °C. Clays Clay Miner. 46, 103–109.

AlDahan, A.A., Morad, S., 1988. Some remarks on the stability of sphene in diagenetic environments. Chem. Geol. 70, 249–255.

Alekseeva, V.A., Hounslow, M.W., 2004. Clastic sediment source characterization using discrete and included magnetic particles—their relationship to conventional petrographic methods in early Pleistocene fluvial–glacial sediments, Upper Don River Basin (Russia). Phys. Chem. Earth 29, 961–971.

Aleva, G.J.J., 1985. Indonesian fluvial cassiterite placers and their genetic environment. J. Geol. Soc. London 142, 815–836.

Anand, R.R., Gilkes, R.J., 1984. Weathering of hornblende, plagioclase and chlorite in meta-dolerite, Australia. Geoderma 34, 261–280.

Antunes, I.M.H.R., Neiva, A.M.R., Silva, M.M.V.G., 2002. The mineralized veins and the impact of old mine workings on the environment at Segura, central Portugal. Chem. Geol. 190, 417–431.

Basu, A., Molinaroli, E., 1989. Provenance characteristics of detrital opaque Fe–Ti oxide minerals. J. Sediment. Petrol. 59, 922–934.

Berner, R.A., Sjöberg, E.L., Velbel, M.A., Krom, M.D., 1980. Dissolution of pyroxenes and amphiboles during weathering. Science 207, 1205–1206.

Borger, H., Burger, D., Kubiniok, J., 1993. Verwitterungsprozesse und deren Wandel im Zeitraum Tertiär—Quartär. Z. Geomorphol. N.F. 37, 129–143.

Bremer, H., 1977. Reliefgenerationen in den feuchten Tropen. Würzbg. Geogr. Arb. 45, 25–38.

Buedel J. Klima-Geomorphologie. Gebrüder Bornträger Berlin—Stuttgart, 1977. 304 pp.

Camm, G.S., Hosking, K.F.D., 1985. Stanniferous placer development on an evolving landsurface with special reference to placers near St. Austell, Cornwall. J. Geol. Soc. London 142, 803–813.

Černy, P., 1992. Geochemical and petrogenetic features of mineralization in rare-element granitic pegmatites in the light of current research. Appl. Geochem. 7, 393–416.

Černy, P., Chapman, R., Simmons, W.B., Chackowsky, E., 1999. Niobian rutile from the McGuire granitic pegmatite, Park County, Colorado: Solid solution, exsolution, and oxidation. Am. Mineral. 84, 754–763.

Coakley, G.J., Mobbs, P.M., 1998. The mineral industry of Malawi. Mineral industries of Africa and the Middle East. US Geol. Survey Minerals Yearbook 2001, vol. 3, pp. 29.1–29.2.

Corbett, I., Burrell, B., 2003. The earliest Pleistocene (?) Orange River fan-delta: an example of successful exploration delivery aided by applied Quaternary research in diamond placer sedimentology and paleontology. Quat. Int. 82, 63–73.

De Jong, J.D., Van der Walls, L., 1971. Depositional environment and weathering phenomena of the white Miocene sands of southern Limburg (the Netherlands). Geol. Mijnb. 50, 417–424.

De Wit, M.C.J., 1999. Post-Gondwana drainage and the development of diamond placers in western South Africa. Econ. Geol. 94, 721–740.

Dill, H.G., 1985. Die Vererzung am Westrand der Böhmischen Masse.—Metallogenese in einer ensialischen Orogenzone. Geol. Jahrb., Reihe D Mineral. Petrogr. Geochem. Lagerstattenkd. 73, 3–461.

Dill, H.G., 1989. Facies and provenance analysis of Upper Carboniferous to Lower Permian fan sequences at a convergent plate margin, using phyllosilicates, heavy minerals and rock fragments (Erbendorf Trough, F.R. of Germany). Sediment. Geol. 61, 95–110.

Dill, H.G., 1995. Heavy mineral response to the progradation of an alluvial fan: implication concerning unroofing of source area, chemical weathering, and paleo-relief (Upper Cretaceous Parkstein fan complex/SE Germany). Sediment. Geol. 95, 39–56.

Dill, H.G., 1998. A review of heavy minerals in clastic sediments with case studies from the alluvial-fan through the nearshore-marine environments. Earth-Sci. Rev. 45, 103–132.

Dill, H.G., 2001. The geology of aluminum phosphates and sulphates of the alunite supergoup: A review. Earth-Sci. Rev. 53, 25–93.

Dill, H.G., Busch, K., Blum, N., 1991. Chemistry and origin of veinlike phosphate mineralization, Nuba Mts. (Sudan). Ore Geol. Rev. 6, 9–24.

Dill, H.G., Fricke, A., Henning, K.H., 1995. The origin of Ba- and REE-bearing aluminium–phosphate–sulphate minerals from the Lohrheim kaolinitic clay deposit (Rheinisches Schiefergebirge, Germany). Appl. Clay Sci. 10, 231–245.

Dill, H.G., Ludwig, R.R., Kathewera, A., Mwenelupembe, J.A.A., 2005. Lithofacies terrain model for the Blantyre Region: Implications for the interpretation of palaeosavanna depositional systems and for environmental geology and economic geology in southern Malawi. J. Afr. Earth Sci.

Eberl, D.D., Hower, J., 1975. Kaolinite synthesis: the role of the Si/Al and (alkali)/(H^+) ratio in hydrothermal synthesis. Clays Clay Miner. 23, 301–309.

Fletcher, W.K., Loh, C.H., 1996. Transport equivalence of cassiterite and its application to stream sediment surveys for heavy minerals. J. Geochem. Explor. 56, 47–57.

Flügel, E., 1982. Microfacies Analysis of Limestones. Springer, Berlin. 633 pp.

Forster, A., 1965. Erläuterungen zur geologischen Karte von Bayern 1:25000 Blatt Nr. 6340/6341 Vohenstrauss/Frankenreuth. Bayerisches Geologisches Landesamt, München. 174 pp.

Franke, W., 1989. The geological framework of the KTB drill site, Oberpfalz. In: Emmermann, R., Wohlenberg, J. (Eds.), The German Continental Deep Drilling Program (KTB). Springer, Heidelberg, pp. 37–54.

French, H.M., Guglielmin, M., 1999. Observations on the ice-marginal, periglacial geomorphology of Terra Nova Bay, northern Victoria Land, Antarctica. Permafr. Periglac. Process. 10, 331–347.

Friis, H., Nielsen, O.B., Friis, E.M., Balme, B.E., 1980. Sedimentological and palaeobotanical investigations of a Miocene sequence at Lavsbjery, Central Jütland, Denmark. Dan. Geol. Unders. 1979, 51–67.

Frost, M.T., Grey, I.E., Harrowfield, I.R., Mason, K., 1983. The dependence of alumina and silica contents on the extent of alteration of weathered ilmenites from Western Australia. Mineral. Mag. 47, 201–208.

Gardner, L.R., 1980. Mobilization of Al and Ti during weathering—isovolumetric geochemical evidence. Chem. Geol. 30, 151–165.

Hak, J., Johan, Z., Kvacek, M., Liebscher, W., 1969. Kemmlitzite a new mineral of the woodhouseite group. N. Jb. Mineral. Mh. 1969, 201–212.

Howard, K.J., Fisk, M.R., 1988. Hydrothermal alumina-rich clays and boehmite on the Gorda Ridge. Geochim. Cosmochim. Acta 52, 2269–2279.

Hubert, J.F., 1962. A zircon–tourmaline–rutile maturity index and the interdependence of the composition of heavy-mineral assemblages with the gross composition and texture of sandstones. J. Sediment. Petrol. 32, 440–450.

Huertas, F.J., Fiore, S., Huertas, F., Linares, J., 1999. Experimental study of the hydrothermal formation of kaolinite. Chem. Geol. 156, 171–190.

Illenberger, W., 1991. Pebble shape (and size!). J. Sediment. Petrol. 61, 756–767.

Louis, H., 1984. Zur Reliefentwicklung der Oberpfalz. Relief Boden Paläoklima 3, 1–66.

Mange, M.A., Maurer, H.F.W., 1991. Schwerminerale in Farbe. Enke, Stuttgart. 150 pp.

Ministry of Energy and Mining, 1997. Mineral Potential of Malawi-Opportunities for Investment. Malawi, Ministry of Energy and Mines, Lilongwe. 14 pp.

Möller, P., Dulski, P., Szacki, W., Malow, G., Riedel, E., 1988. Substitution of tin in cassiterite by tantalum, niobium, tungsten, iron and manganese. Geochim. Cosmochim. Acta 52, 1497–1503.

Morton, A.C., 1984. Stability of detrital HM in Tertiary sandstones from the North Sea basin. Clay Miner. 19, 287–308.

Morton, A.C., 1991. Geochemical studies of detrital heavy minerals and their application to provenance research. In: Morton, A.C., Todd, S.P., Haughton, P.D.W. (Eds.), Developments in Sedimentary Provenance Studies. Geological Society Special Publications, vol. 57. The Geological Society, London, pp. 31–45.

Morton, A.C., Hallsworth, C.R., 1994. Identifying provenance-specific features of detrital heavy mineral assemblages in sandstones. Sediment. Geol. 90, 241–256.

Mücke, A., Bhadra Chaudhuri, J.N., 1991. The continuous alteration of ilmenite through pseudorutile to leucoxene. Ore Geol. Rev. 6, 25–44.

Mücke, A., Keck, E., Haase, J., 1990. Die genetische Entwicklung des Pegmatits von Hagendorf-Süd/Oberpfalz. Der Aufschluss 41, 33–51.

Nickel, E., 1973. Experimental dissolution of light and heavy-minerals in comparison with weathering and intrastratal solution. Contrib. Sedimentol. 1, 1–68.

Pettijohn, F.J., 1941. Persistence of heavy minerals and geologic age. J. Geol. 49, 610–625.

Putter, T.D., Andre, L., Bernard, A., Dupuis, C., Jedwab, J., Nicaise, D., Perruchot, A., 2002. Trace element (Th, U, Pb, REE) behavior in a cryptokarstic halloysite and kaolinite deposit from Southern Belgium: importance of “accessory” mineral formation for radioactive pollutant trapping. Appl. Geochem. 17, 1313–1328.

Ramdohr, P., 1975. Die Erzminerale und ihre Verwachsungen. Akademie-Verlag, Berlin. 1277 pp.

Raufuss, W., 1973. Struktur, Schwermineralführung, Genese und Bergbau der sedimentären Rutil-Lagerstätten in Sierra Leone (Westafrika). Geol. Jahrb., Reihe D Mineral. Petrogr. Geochem. Lagerstattenkd. 5, 1–52.

Salger, M., 1985. Schwer-und Tonminerale des Keupers in der Forschungsbohrung Obernsees. Geol. Bav. 88, 143–147.

Schnitzer, W.A., 1957. Die Lithologie und Paläogeographie am Westrand der Böhmischen Masse. Erlanger Geol. Abh. 5, 1–130.

Smith, D.J., 1992. Long-term rates of contemporary solifluction in the Canadian Rocky Mountains. In: Dixon, J.C., Abrahams, A.D. (Eds.), Periglacial Geomorphology. Wiley, Chichester, pp. 203–221.

Stanaway, K.J., 1992. Heavy mineral placers. Min. Eng. 44, 352–358.

Störr, M., 1975. Kaolin deposits of the GDR in the Northern Region of the Bohemian Massif. Ernst-Moritz-Arndt University Greifswald. 243 pp.

Störr, M., Köster, H.M., Kromer, H., Hilz, M., 1991. Minerale der Crandallit-Reihe im Kaolin von Hirschau-Schnaittenbach, Oberpfalz. Z. Geol. Wiss. 19, 677–683.

Strunz, H., Forster, A., Tennyson, Ch., 1975. Die Pegmatite der nördlichen Oberpfalz. Aufschluss, Special Paper 26, 117–189.

Thomas, M.F., 1994. Geomorphology in the Tropics. Wiley, Chichester. 460 pp.

Tillmanns, W., 1978. Sedimentpetrographische Untersuchungen an Doggersandstein und oberkretazischen Sedimenten auf Blatt Hirschau (Oberpfalz). Geol. Bl. NO-Bayern 28, 227–242.

Tricart, J., Cailleux, A., 1958. Cours de Geomorphologie I: Geomorphologie Structurale. C.D.U, Paris. 252 pp.

Trusheim, F., 1936. Die geologische Geschichte Süddeutschlands während der Unterkreide und des Cenomans. Neues Jahrb. Mineral. 75, 2–108 (supplementary volume Sect. B).

Twidale, C.R., 2002. The two-stage concept of landform and landscape development involving etching: origin, development and implications of an idea. Earth-Sci. Rev. 57, 37–74.

Velbel, M.A., 1989. Weathering of hornblende to ferruginous products by a dissolution–reprecipitation mechanism: petrography and stoichiometry. Clays Clay Miner. 37, 515–524.

Washburn, L., 1999. A High Arctic frost-creep/gelifluction slope, 1981–89: Resolute Bay, Cornwallis Island, Northwest Territories, Canada. Permafr. Periglac. Process. 10, 163–186.

Winterbottom, S.J., 2000. Medium and short-term channel planform changes on the Rivers Tay and Tummel, Scotland. Geomorphology 34, 195–208.

Yim, W.W.S., 1994. Particle size and trace element distribution characteristics of cassiterite as an aid to provenance study of stanniferous placers in northeastern Tasmania. Aust. J. Southeast Asian Earth Sci. 10, 131–142.

Zack, T., Kronz, A., Foley, S., Rivers, T., 2002. Trace element abundances in rutiles from eclogites and associated garnet mica schists. Chem. Geol. 184, 97–122.

Zack, T., von Eynatten, H., Kronz, A., 2004. Rutile geochemistry and its potential use in quantitative provenance studies. Sediment. Geol. 171, 37–58.